JOURNAL OF SOLID STATE CHEMISTRY **75**, 381–389 (1988)

Defect Model and Transport at High Temperature in $YBa_2Cu_3O_{6+Y}$

M.-Y. SU, S. E. DORRIS, AND T. O. MASON

Northwestern University, Department of Materials Science and Engineering and Materials Research Center, The Technological Institute, Evanston, Illinois 60208

Received December 30, 1987

From 650–850°C *in situ* conductivity and thermopower measurements it was determined that $YBa_2Cu_3O_{6+Y}$ is a *p*-type small polaron conductor over the range $0.15 \le y \le 0.75$ with a hopping energy of approximately 0.1 eV. Copper valence distribution on the Cu(1) site was calculated from the thermopower and literature values for the oxygen content, Y. All three valence state of Cu appear to be present with the equilibrium constant of disproportionation,

$$2Cu^{2+} \Leftrightarrow Cu^{+} + Cu^{3+},$$

independent of temperature and oxygen content. The defect model proposed to explain the nonstoichiometry and transport behavior is:

$$Cu^{+} + \tfrac{1}{2}O_2(g) \Leftrightarrow O_O^{=} + Cu^{3+}.$$

As $Y \rightarrow 0$ at low p_{O_2}, a *p*-to-*n* transition is detected, possibly indicating a Cu^{+}/Cu^{2+} e^{-}-type small polaron mechanism as opposed to the Cu^{3+}/Cu^{2+} *h*-type mechanism over most values of Y. The phase boundary at low p_{O_2} prevents further investigation of this *n*-type mechanism.

Introduction

As discussed by Sleight (*1*), oxygenated Y_{123} ($YBa_2Cu_3O_7$) should really be considered an intercalation of oxygen in $YBa_2Cu_3O_6$, the stable form at elevated temperature. We therefore chose to represent the oxygen content as Y in $YBa_2Cu_3O_{6+Y}$. Fueki *et al.* (*2*) and Gallagher (*3*) have documented the change in oxygen content with oxygen partial pressure over the range of interest to this study. Although suggestions have been made concerning the defect structure (*4*), to date the defect model has not been established.

The defect structure is known to play the dominant role in achieving superconductivity in Y_{123}. It is widely appreciated that ordering of oxygen along chains with copper in Cu(1) positions not only determines the crystal symmetry (tetragonal vs orthorhombic) but is necessary to achieve superconductivity. It is therefore of interest to investigate the defect structure at high temperature, where processing and oxygenation of Y_{123} take place. The defect structure not only determines the equilibrium oxygen content at a given set of conditions (T, p_{O_2}) but also the rates of oxidation/reduction through oxygen/defect mobilities which vary with the oxygen content.

It is also important to characterize the normal state electrical behavior in Y_{123}. By performing measurements where point de-

0022-4596/88 $3.00

fect equilibrium is achieved, it is possible to separate the temperature dependence of the density of carriers from that of the mobility. Considerable confusion has resulted from the temperature dependence of resistivity (or conductivity) under fixed p_{O_2} at high temperature. Under such conditions, the oxygen content decreases markedly with increasing temperature (*2, 3*); the hole population decreases proportionately, as we will demonstrate. By properly analyzing the temperature and concentration dependence of the mobility, we will show that small polaron conduction is operative at high temperature over a broad range of oxygen content in both tetragonal and orthorhombic phases. This indicates that electron–phonon interactions are strong, at least at high temperature, a fact which may be relevant to models for superconductivity.

Experimental

At the inception of this study, single crystals large enough for four point high-temperature electrical measurements were unavailable. Instead highly dense (>95%), textured specimens of Y_{123} were prepared by sinter-forging of powders derived from solid-state reactions of high purity Y_2O_3, CuO, and $BaCO_3$. Processing conditions are given elsewhere (*5*). The microstructure obtained consisted of approximately 50 by 50 by 5- to 10-μm crystallites whose plate normals (and *c*-axes) were oriented parallel to the forging axis. Rectangular bars (2 by 2 by 15 mm) were cut perpendicular to the direction of *c*-axis preference; measurements were therefore performed parallel to the *a–b* planes of the crystallites.

Four point simultaneous conductivity and thermopower measurements were performed in the apparatus described previously (*6*). Flowing O_2 and O_2/Ar mixtures were used to achieve oxygen partial pressures over the range 10^{-4} to 10^{0}. Pt/Rh thermocouples were employed. All measurements were reversible; no evidence of reaction between the thermocouples and the sample was seen. Thermopowers were corrected for the contribution of the thermocouple leads; conductivity was corrected for thermal emf by a standard current reversal procedure.

Due to the large crystallite size within the sample, rather long equilibration times were observed. Conductivity was continuously monitored as a function of time to establish relaxation times. These were as long as 4 days at the lowest temperatures (650°C) and as short as a few hours at the highest temperature (850°C). At the end of the experimental campaign, a few experiments were carried out below $p_{O_2} = 10^{-4}$ at 850°C. A plateau was obtained for both electrical properties, indicative of the decomposition which has been documented by Ahn *et al.* (*7*) as occurring at

$$\log p_{O_2}(\mathrm{atm}) = 4.57 - 8502/T. \qquad (1)$$

Our results would place the boundary somewhat lower in p_{O_2} space at 850 and 770°C. The sluggish kinetics associated with our large-grained sample prevented the collection of more closely spaced points in order to more precisely fix the decomposition boundary.

Results

Electrical conductivity and thermopower data are given in Figs. 1 and 2, respectively. The absolute values and trends are in good agreement with the data being generated by a number of other groups (*8–11*) with the possible exception of Anderson *et al.* (*12*) who obtained shallower oxygen partial pressure dependencies for both properties. In general, *p*-type behavior is seen over much of the stability range examined, with a hint of a transition to *n*-type behavior at low p_{O_2}. Choi *et al.* (*9*) have also reported indications of *n*-type behavior at low p_{O_2}.

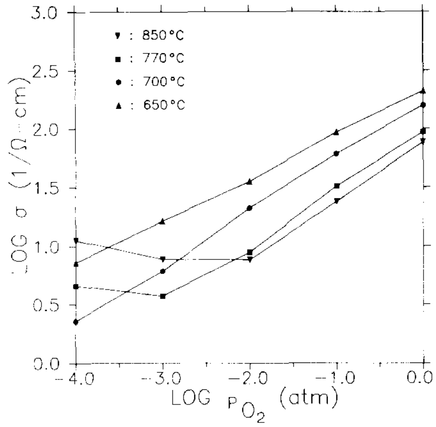

FIG. 1. Experimental conductivity vs oxygen partial pressure.

The overall behavior in Y_{123} is indicative of semiconductive behavior; conductivity is too small and thermopower too large for metallic behavior. The large oxygen partial pressure dependence of both properties is also characteristic of a semiconductor where carrier density varies with the defect content.

What is unusual about the defect-related properties of Y_{123} at high temperature is the difference between their oxygen partial pressure dependencies (see Table I). Whereas the oxygen exponent of the conductivity is typically $\frac{1}{2}$, the exponent for the thermopower is $\frac{1}{3}$ or smaller, and the exponent for the oxygen excess (Y) is smaller still. Furthermore, the oxygen exponents of the electrical properties have the opposite temperature dependence from that of the oxygen content. It is apparent that a simple point defect model involving oxygen vacancies with various effective charge states compensated by free carriers cannot explain these anomalies. As was shown previously, divergence in the slopes of conductivity and thermopower can be obtained when small polaron conduction is operative (*13*). Therefore, an analysis of the conduction mechanism was carried out.

TABLE I

INVERSE OXYGEN EXPONENTS OVER THE RANGE $-1 \leq \log p_{O_2} \leq 0$ IN $YBa_2Cu_3O_{6-Y}$

T (°C)	$\left(\frac{\partial \log Y}{\partial \log p_{O_2}}\right)^{-1}$	$\left(\frac{\partial \log \sigma}{\partial \log p_{O_2}}\right)^{-1}$	$\left(\frac{\partial \frac{-Q}{2.303k/e}}{\partial \log p_{O_2}}\right)^{-1}$
650	5.06[a]	2.86	6.01
700	6.61[a]	2.43	4.61
850	8.54[a]	1.98	3.31

[a] From the data of Fueki *et al.* (*2*).

Conduction Mechanism Analysis

The main identifying characteristic of small polaron conduction is an activated mobility. To determine the temperature dependence of the mobility in a given regime, it is necessary to carry out the analysis at constant carrier concentration. It is not enough that this be done at constant defect concentration; neutral species can ionize at constant defect content producing more charge carriers. Instead, conductivities on several isotherms but at constant thermopower can be compared (*14*). This has been done at thermopower values of 150 and 90 μV/K in Fig. 3. A small polaron hopping

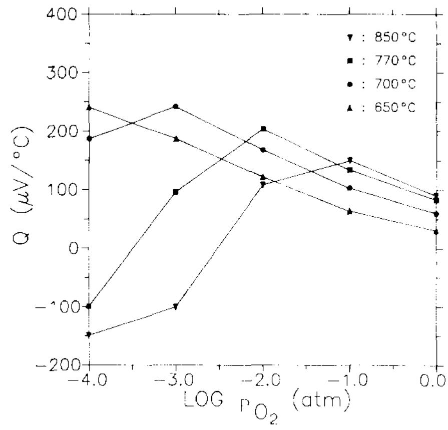

FIG. 2. Experimental thermopower vs oxygen partial pressure.

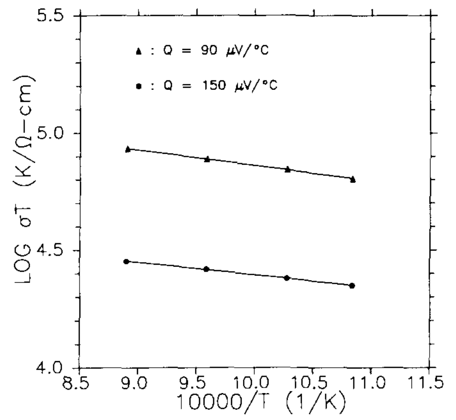

FIG. 3. Isothermoelectric analysis of conductivity showing an activated mobility.

energy of approximately 0.1 eV is obtained and appears to be independent of oxygen content over the range of Y values involved in the analysis, i.e., 0.25 to 0.52. A similar analysis but at constant values of Y yields virtually identical activation energies; there is apparently little additional production of charge carriers at constant oxygen content. The carrier concentration (or the valence ratio for small polaron conduction) is uniquely determined by the oxygen content, independent of temperature. A similar conclusion was reached by Sageev-Grader *et al.* (*8*). The activation energy in Y_{123} compares favorably with other small polaron transition metal oxide conductors, e.g., Fe_3O_4 (0.11 eV) (*15*), FeO (0.16 eV) (*16*), and $La_{1-x}Sr_xCrO_3$ (0.11–0.19 eV) (*17*).

A second distinguishing characteristic feature of small polaron conduction is a composition-dependent mobility (*15–17*),

$$\mu = \frac{(1 - c')ge^2a^2\nu}{kT} \exp\left[\frac{-E_H}{kT}\right], \tag{2}$$

where g is a geometric factor, e is the charge on the electron, a is the jump distance, ν is the vibrational frequency, E_H is the hopping energy, k is Boltzmann's constant, and T is temperature. The $(1 - c')$ term is related to the site fraction of carriers, c', and gives the probability that neighboring species on equivalent sites are of appropriate charge for transfer of the polaron to take place, i.e., Cu^{3+} to Cu^{2+}. The carrier concentration would be the product of N, the combined density of Cu^{3+} and Cu^{2+} on conducting sites, and c'. Since the hole population closely follows the oxygen content, a simple test for the $(1 - c')$ term can be made by examining the quotient of conductivity and oxygen content. As can be seen in Table II, there is definitely a composition dependence of the mobility.

Defect and Thermopower Model

Cooper *et al.* (*18*) reported that the normal state thermopower in $La_{2-x}M_xCuO_4$ (M = Ba or Sr) obeyed the Heikes–Chaikin–Beni small polaron equation (*19*),

$$Q = -\frac{k}{|e|} \ln 2 \frac{[Cu^{3+}]}{[Cu^{2+}]}, \tag{3}$$

where k is Boltzmann's constant, e is the charge on the electron, and the $[Cu^{3+}]$ represents the concentration of localized holes needed to charge compensate the Ba or Sr dopant. Given the activated mobility in Y_{123}, discrete Cu^{3+} species can also be postulated in this oxide. In the following model, it will be assumed that the Cu(2) site is occupied exclusively by Cu^{2+} and that all three valence states reported in Y_{123} can occur simultaneously on the Cu(1) site. The formula unit can then be represented by

$$Y^{3+}Ba_2^{2+}(Cu_2^{2+})\{Cu_a^{+}Cu_b^{2+}Cu_c^{3+}\}O_{6+Y}, \tag{4}$$

where species on the Cu(2) and Cu(1) sites are enclosed by ( ) and { }, respectively. The Cu(1) site balance is simply

$$a + b + c = 1, \tag{5}$$

and the charge balance, assuming formal charges (see Ref. (*20*) for a discussion of formal vs real charge), is given by:

$$a + 2b + 3c = 2(6 + Y) - 11. \tag{6}$$

TABLE II

EXPERIMENTAL RESULTS AND CALCULATIONS

T °K	$\log p_{O_2}$ (atm)	σ $(\Omega\ \mathrm{cm})^{-1}$	Q $(\mu V/K)$	Y[a]	σ/Y	a	b	c	K_D[b]	K_{ox}[c]	σ/α[d]	σ/β[e]
650	−4	7.3	241	0.150	48.7	0.730	0.241	0.029	0.364	3.97	282	1878
	−3	16.4	187	0.280	58.6	0.528	0.385	0.088	0.312	5.25	230	821
	−2	35.7	122	0.430	83.0	0.352	0.436	0.212	0.393	6.03	251	583
	−1	93.9	64	0.590	159.2	0.207	0.407	0.387	0.484	5.93	473	803
	0	209.2	31	0.750	278.9	0.052	0.396	0.552	0.183	10.62	907	1210
700	−3	6.14	242	0.195	31.5	0.648	0.314	0.038	0.249	1.85	181	930
	−2	21.7	168	0.340	63.8	0.443	0.433	0.123	0.291	2.78	226	665
	−1	61.1	103	0.495	123.4	0.281	0.448	0.271	0.379	3.04	362	731
	0	157.6	60	0.635	248.2	0.153	0.424	0.423	0.359	2.77	744	1172
770	−2	8.95	204	0.240	37.3	0.585	0.344	0.065	0.314	1.12	163	677
	−1	32.5	134	0.395	82.3	0.391	0.428	0.181	0.385	1.46	255	646
	0	92.7	83	0.555	167.0	0.225	0.439	0.335	0.391	1.44	488	879
850	−1	24.2	150	0.30	80.7	0.524	0.353	0.124	0.521	0.747	264	895
	0	76.6	90	0.42	182.4	0.406	0.349	0.245	0.817	0.605	532	1266

[a] Y in $Y^{3+}Ba^{2+}(Cu_2^{2+})\{Cu_a^{+}Cu_b^{2+}Cu_c^{3+}\}O_{6+Y}$ from Fueki *et al.* (2).

[b] $K_D = ac/b^2$.

[c] $K_{ox} = c/(ap_{O_2}^{1/2})$.

[d] $\alpha = bc/(b + c)$.

[e] $\beta = \alpha Y$.

Combining Eqs. (5) and (6) yields:

$$b + 2c = 2Y. \tag{7}$$

If no monovalent copper existed ($b + c = 1$), Eq. (7) could be solved directly for b and c, the divalent and trivalent copper contents. Using the data of Fueki et al. (2) for Y, these concentrations and the corresponding thermopowers according to Eq. (3) were calculated. Also, a second small polaron model for thermopower was examined:

$$Q = \frac{k}{e} \ln 2 \frac{[Cu^{2+}]}{[Cu^{3+}]}. \tag{8}$$

This model has been successfully employed to describe Cr^{4+}/Cr^{3+} small polaron conduction in $La_{1-x}Sr_xCrO_3$ (*17*) and Mn^{4+}/Mn^{3+} small polaron conduction in cubic Mn_3O_4 (*21*). In neither case does the thermopower calculated from the oxygen contents of Fueki *et al.* (*2*) agree with the measured values in Fig. 2; monovalent copper must be incorporated in the model.

From the thermopower and oxygen content, all three copper valence concentrations per formula unit were calculated from Eqs. (3) and (7) (e^--type polaron, Cu^{2+}) or from Eqs. (7) and (8) (h^+-type polaron, Cu^{3+}). In the first case, real solutions could not be obtained for values of Y greater than 0.5. Furthermore, Cu^{3+} concentrations were typically quite small ($Y \leq 0.2$) and the degree of Cu^{2+} disproportionation according to

$$2Cu^{2+} \Leftrightarrow Cu^{+} + Cu^{3+} \tag{9}$$

was strongly temperature dependent. As will be discussed below, high-temperature XANES suggests that the degree of disproportionation is temperature-independent (*22*).

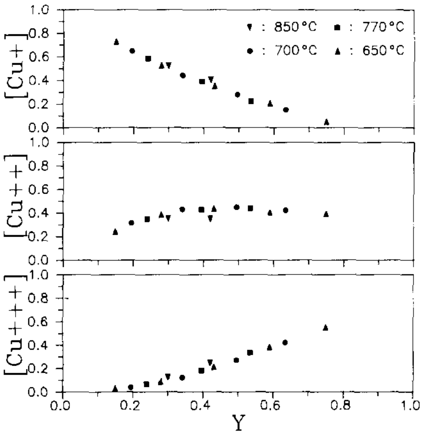

FIG. 4. Copper species concentrations on Cu(1) sites vs Y in $YBa_2Cu_3O_{6+Y}$.

In contrast, the h^+-type small polaron model (Eq. (8)) yielded physically real solutions at every value of oxygen content (see Table II). Results vs oxygen content for all four experimental isotherms are superimposed in Fig. 4. Trivalent copper increases with increasing oxygen content whereas monovalent copper decreases. Divalent copper is approximately invariant. This indicates that the disproportionation constant of Eq. (9) is independent of composition. The fact that the species concentrations for all four isotherms superimpose suggests that K_D is also independent of temperature in the temperature range of our experiments. This is borne out in Table II. It is interesting to note that the XANES spectra of oxygenated Y_{123} which indicate average valence of copper between CuO and KCu O_2 are temperature-independent over the temperature range 4 to 688 (*22*). This result is consistent with our results.

Defect Model and Conduction Parameters

A proposed defect model consistent with the oxygen partial pressure dependence of the thermopower and oxygen content is:

$$Cu^+ + \tfrac{1}{2}O(g) \Leftrightarrow O_0^= + Cu^{3+}. \qquad (10)$$

Similar models have been proposed by Gallagher (*3*) on the basis of TGA data, Morss and Thorn (*23*) on the basis of solution calorimetry, and Han and Monroe (*10*) on the basis of TGA and conductivity. Real charges have been written for the ions as opposed to effective charges on defects. If one takes $[O_0^=]$ at approximately unit activity, i.e., $[O_0^=] \cong (6 + Y)/7$, for example, equilibrium constants are obtained for Eq. (10) which are approximately composition-independent at each temperature and which decrease slightly with increasing temperature (see Table II). This temperature dependence can be expressed as:

$$\ln K_{ox} = -10.08 + 10885/T. \qquad (11)$$

In this calculation, the average of K_{ox} at each temperature of values within ±10% of that average were employed. In general, data at thermopowers in excess of 200 are suspect due to the incipient transition to n-type behavior and were not included in the calculation.

Combining the definition of small polaron carrier concentration, $p = Nc'$, with that of the mobility (Eq. (2)), we obtain:

$$\sigma = Nc'(1 - c')\left[\frac{ge^2a^2\nu}{k}\right]T^{-1}\exp\left[\frac{-E_H}{kT}\right]. \qquad (12)$$

It can be shown that the first term in Eq. (12) written in terms of the Cu(1) site occupancies is:

$$Nc'(1 - c') = [bc/(b + c)]N_{FU} \qquad (13)$$

where N_{FU} is the density of formula units (cm^{-3}). Combining N_{FU} with the second term in Eq. (12) and assuming that this term is approximately composition- and temperature-independent, it follows that:

$$\sigma = \frac{bc}{(b + c)}\sigma_0 T^{-1}\exp\left[\frac{-E_H}{kT}\right]. \qquad (14)$$

For each isotherm σ/α, where $\alpha = bc/(b + c)$, ought to be constant. This is not seen in

Table II. Instead, it can be shown than σ/β, where $\beta = \alpha Y$, is approximately constant. This indicates that the jump probability is not simply $(1 - c')$ in Eq. (2), which would be the conduction site fraction of Cu^{2+}, but rather the product of this term and the oxygen content, Y. This is reasonable considering that an oxygen ion would be required between two adjacent Cu(1) sites in order for an exchange to take place. Therefore, the probability of conduction is proportional to the product of the Cu^{2+} site fraction (Cu(1) site) and the fractional occupation of adjacent oxygen sites. This explains why the conductivity has a larger oxygen exponent than the thermopower or oxygen content (see Table I). In fact, the oxygen exponent of conductivity is approximately the sum of those for the thermopower and the oxygen content.

Assuming the defect model to be correct, conduction parameters can be calculated from the electrical conductivity. The density of holes is $N_{FU}c'$ or $N_{FU}c/(b + c)$ and varies over the range 6.5×10^{20} to 3.5×10^{21}. It should be emphasized that this is for a range of oxygen contents from 0.15 to 0.75; hole content would be even higher in well-oxygenated material. Normal state Hall effect (*24*) and thermal conductivity (*25*) in oxygen-rich Y_{123} indicate hole populations in the 1–6 × 10^{21} range. Mobilities calculated from the measured conductivities and calculated hole concentrations range from 0.07 to 0.37 $cm^2\ v^{-1}s^{-1}$, values once again typical for small polaron conductors (*15–17*). As a final confirmation, the lattice vibrational frequency in Eq. (12) was calculated assuming $g = 1$ and $a = 3.8$ Å. A value of $\approx 1 \times 10^{14}\ sec^{-1}$ was obtained. Very similar values occur in other small polaron systems (*15–17*).

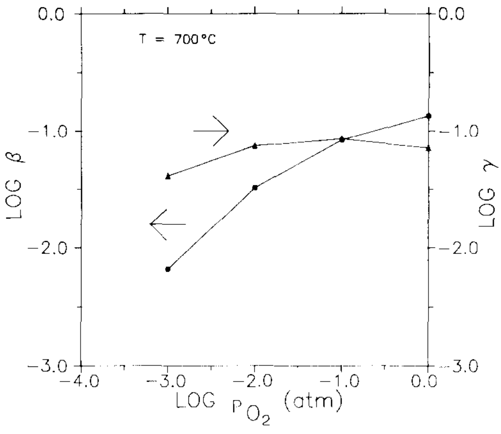

FIG. 5. Predicted oxygen partial pressure dependencies for *p*-type (β) and *n*-type (γ) small polaron mechanisms. See text for explanation.

In addition to describing the electrical properties in the *p*-type regime at large Y, the valence distributions in Fig. 4 also suggest an explanation for the transition to *n*-type behavior at small Y. In Fig. 5, both $\beta = Ybc/(b + c)$ and $\gamma = Yab/(a + b)$ have been plotted on a log scale vs oxygen partial pressure. The γ term would correspond to an e^--type small polaron mechanism involving Cu^+ and Cu^{2+} on Cu(1) sites and mediated by the oxygen ions between them. The nearly $\frac{1}{2}$ slope of β, which governs *p*-type conductivity, is clearly evident. In contrast, γ has nearly zero slope due to the cancellation of Y vs p_{O_2} and $\alpha = [Cu^+]$ vs p_{O_2}. This can explain why the *p*-to-*n* transition is so gradual and why the *n*-type regime is not pronounced. (Except for the Y dependence of the two mechanisms, one would expect a transition near $Y = 0.5$, assuming that the hopping energies are nearly the same.)

Conclusion

We have shown that the high-temperature electrical properties of Y_{123} are adequately described by a model involving Cu^+, Cu^{2+}, and Cu^{3+} on the Cu(1) site with charge transport taking place via small polaron hopping between Cu^{3+} and Cu^{2+} or between Cu^+ and Cu^{2+}. The strong localization of charge carriers also supports the assignment of formal charge to the cations involved. Corroboration for this is seen in both independent spectroscopic measurements and in theoretical calculations. As cited above, XANES work is consistent with Cu^{3+} at high oxygen contents (*22, 26*) and Cu^{+} in reduced materials (*22, 26, 27*). Very little edge shift as a function of temperature is seen over the range 4–688 K (*22*), an observation also consistent with the results and model of this work. Theoretically, Allan and Mackrodt (*28*) have carried out atomistic calculations showing that both Cu^{+} and Cu^{3+} are stable species in Y_{123} and that Cu^{3+} is energetically more favorable than the O^{-} species. Ramifications for high T_c superconductivity will be considered elsewhere.

Acknowledgments

This work was supported by the Northwestern University Materials Research Center under the N.S.F.-M.R.L. Grant number DMR-8520280. Helpful discussions with D. L. Johnson, C. Kannewurf, and K. R. Poeppelmeier are gratefully acknowledged.

References

1. A. W. Sleight, *in* "Proc. Mater. Res. Soc. Symp., High Temperature Superconductors" **99,** 3 (1988).

2. K. Fueki, K. Kitazawa, K. Kishio, T. Hasegawa, S.-I. Ichida, H. Takagi, and S. Tanaka, *in* "Chemistry of High Temperature Superconductors," p. 38, Amer. Chem. Soc., Washington, DC (1987).

3. P. K. Gallagher, *Adv. Ceram. Mater.* **2**(3B), 632 (1987).

4. J. F. Marucco, C. Noguera, P. Garoche, and G. Collin, *J. Mater. Res.* **2**(6), 757 (1987).

5. Q. Robinson, P. Georgopoulos, D. L. Johnson, H. O. Marcy, C. R. Kannewurf, S.-J. Hwu, T. J. Marks, K. R. Poeppelmeier, S. N. Song, and J. B. Ketterson, *Adv. Ceram. Mater.* **2**(3B), 380 (1987).

6. A. Trestman-Matts, S. E. Dorris, and T. O. Mason, *J. Amer. Ceram. Soc.* **66**(8), 589 (1983).

7. B. T. Ahn, T. M. Gur, R. A. Huggins, R. Beyers, and E. M. Engler, *in* "Proc. Mater. Res. Soc. Symp., High Temperature Superconductors" **99,** 171 (1988).

8. G. Sageev-Grader, P. K. Gallagher, and E. M. Gyorgy, *Appl. Phys. Lett.* **51**(14), 1115 (1987).

9. G. M. Choi, H. L. Tuller, and M. J. Tsai, *in* "Proc. Mater. Res. Soc. Symp., High Temperature Superconductors" **99,** 141 (1988).

10. Y. H. Han and D. W. Monroe, *in* "Proc. Mater. Res. Soc. Symp., High Temperature Superconductors" **99,** 753 (1988).

11. J. Javadpour, C. S. Niou, and N. G. Eror, presented at the Mater. Res. Soc. Symp., High Temperature Superconductors, Nov. 30–Dec. 3, 1987, Boston, MA.

12. H. U. Anderson, C. J. Brannon, and D. M. Sparlin, *in* "Proc. Mater. Res. Soc. Symp., High Temperature Superconductors" **99,** 937 (1988).

13. G. Petot-Ervas, P. Ochin, and T. O. Mason, "Proceedings, 3rd Int. Conf. Transport in Nonstoichiometric Compounds, NATO Adv. Studies Inst., Ser. B: Physics" (G. Simkovich and V. S. Stubican, Eds.), p. 61, Plenum, New York (1985).

14. H.-C. Chem, E. Gartstein, and T. O. Mason, *J. Phys. Chem. Solids* **43**(10), 991 (1982).

15. R. Dieckmann, C. A. Witt, and T. O. Mason, *Ber. Bunsenges. Phys. Chem.* **87**(6), 495 (1983).

16. E. Gartstein and T. O. Mason, *J. Amer. Ceram. Soc.* **65**(2), C24 (1982).

17. D. P. Karim and A. T. Aldred, *Phys. Rev. B* **20,** 2255 (1979).

18. J. R. Cooper, B. Alavi, L.-W. Zhou, W. P. Beyermann, and G. Gruner, *Phys. Rev. B* **35**(16), 8794 (1987).

19. P. M. Chaikin and G. Beni, *Phys. Rev. B* **13,** 647 (1976).

20. A. Sleight, "Chemistry of High Temperature Superconductors," p. 2, Amer. Chem. Soc., Washington, DC (1987).

21. S. E. Dorris and T. O. Mason, *J. Amer. Ceram. Soc.*, in press.

22. J. B. Boyce, F. Bridges, T. Claeson, R. S. Howland, and T. H. Geballe, *in* "Proc. Mater. Res. Soc. Symp., High Temperature Superconductors" **99,** 943 (1988).

23. L. R. Morss and R. J. Thorn, *in* "Proc. Mater. Res. Soc. Symp., High Temperature Superconductors" **99,** 571 (1988).

24. N. Karpe, I. Szymczak, D.-X. Chen, A. Sanchez, J. Nogues, and K. V. Rao, *in* "Proc. Mater. Res. Soc. Symp., High Temperature Superconductors" **99,** 483 (1988).

25. J. Heremans and D. T. Morelli, *in* "Proc. Mater. Res. Soc. Symp., High Temperature Superconductors" **99,** 761 (1988).

26. E. E. Alp, G. K. Shenoy, L. Soderholm, D. G.

HINKS, AND H.-B. SCHÜTTLER, *in* "Proc. Mater. Res. Soc. Symp., High Temperature Superconductors" **99,** 177 (1988).

27. S. M. HEALD, J. M. TRANQUADA, A. R. MOODENBAUGH, AND Y. XU, *in* "Proc. Mater. Res. Soc. Symp., High Temperature Superconductors" **99,** 757 (1988).

28. N. L. ALLAN AND W. C. MACKRODT, *in* "Proc. Mater. Res. Soc. Symp., High Temperature Superconductors" **99,** 797 (1988).